Phase-field modeling of pitting and mechanically-assisted corrosion of Mg alloys for biomedical applications: COMSOL implementation

Sasa Kovacevic[a,*], Wahaaj Ali[b,c], Emilio Martínez-Pañeda[a,*], Javier LLorca[b,d,*]

[a]*Department of Civil and Environmental Engineering, Imperial College London, SW7 2AZ London, UK.*

[b]*IMDEA Materials Institute, C/Eric Kandel 2, 28906 Getafe, Madrid, Spain.*

[c]*Department of Material Science and Engineering, Universidad Carlos III de Madrid, 28911 Leganes, Madrid, Spain.*

[d]*Department of Materials Science, Polytechnic University of Madrid, E. T. S. de Ingenieros de Caminos, 28040 Madrid, Spain.*

Abstract

A phase-field model for simulating the corrosion of Mg alloys in body fluids is developed by Kovacevic et al. (2023) [1]. The model incorporates both Mg dissolution and the transport of Mg ions in solution, naturally predicting the transition from activation-controlled to diffusion-controlled bio-corrosion. In addition to uniform corrosion, the presented framework captures pitting corrosion and accounts for the synergistic effect of aggressive environments and mechanical loading in accelerating corrosion kinetics.

The theoretical formulation of the phase-field model is provided in the original paper [1] while this document provides instructions for its implementation in the finite element software COMSOL Multiphysics. Input files for pitting and mechanically-assisted corrosion are provided for demonstration purposes. If the code developed is used for research or industrial purposes, please cite:

*Corresponding authors

Email addresses: s.kovacevic@imperial.ac.uk (Sasa Kovacevic), e.martinez-paneda@imperial.ac.uk (Emilio Martínez-Pañeda), javier.llorca@upm.es,javier.llorca@imdea.org (Javier LLorca)

1. Mathematical formulation

This section briefly introduces the mathematical formulation of the phase-field model for the biocorrosion of Mg-based alloys in biological fluids. The interested reader is referred to the original paper for more details [1].

The problem formulation is depicted in Fig. 1 and could be summarized as follows. The system consists of a biodegradable Mg alloy in contact with physiological environments that, by composition, mimic body fluids. The system domain Ω includes both the Mg alloy and the corrosive environment. A continuous phase-field parameter ϕ is introduced to distinguish different phases: $\phi = 1$ represents the solid phase (Mg alloy), $\phi = 0$ corresponds to the liquid phase (physiological fluid), and $0 < \phi < 1$ indicates the thin interfacial region between the phases (solid-liquid interface). With vanishing normal fluxes ($\mathbf{n} \cdot \mathbf{J} = 0$) on the domain boundary $\partial \Omega$, the independent kinematic variables necessary for model description are the non-conserved phase-field parameter describing the evolution of the corroding interface $\phi(\mathbf{x}, t)$, the displacement vector to characterize deformation of the solid phase $\mathbf{u}(\mathbf{x}, t)$, and the normalized concentration of Mg ions $\bar{c}_{Mg}(\mathbf{x}, t)$ with respect to the concentration in the solid phase ($\bar{c}_{Mg} = c_{Mg}/c_{Mg}^s$).
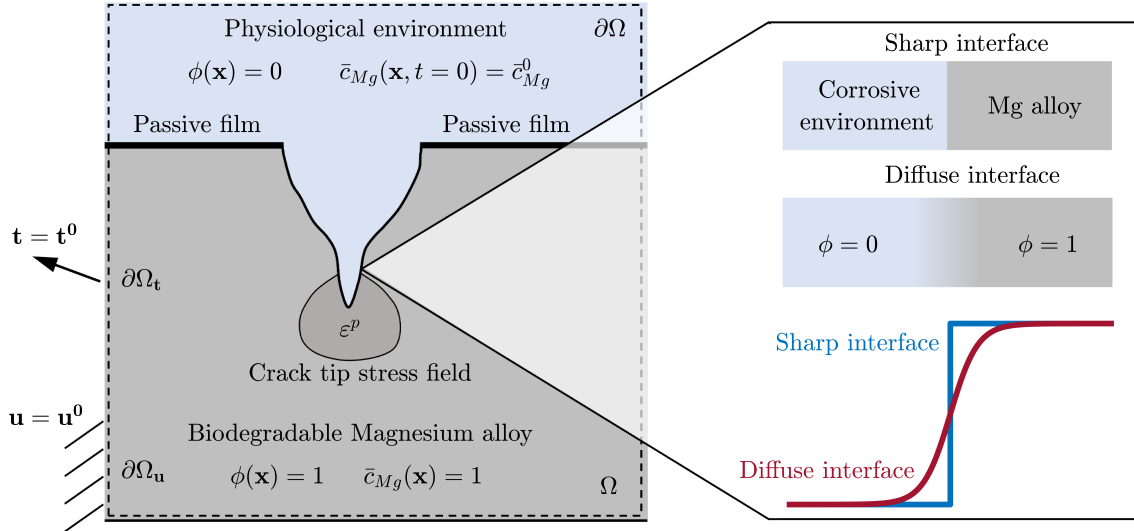

Figure 1: Problem formulation and diffuse interface description of the liquid (physiological environment $\phi = 0$) and solid (biodegradable Mg alloy $\phi = 1$) phases.

The free energy functional for a heterogeneous system such as the one in Fig. 1 can be written as

$$\mathscr{F} = \int_{\Omega} \left[f^{chem}(\bar{c}_{Mg}, \phi) + f^{grad}(\nabla \phi) + f^{mech}(\nabla \mathbf{u}, \phi) \right] d\Omega, \tag{1}$$

where f^{chem}, f^{grad}, and f^{mech} are the chemical, gradient, and mechanical energy densities defined below.

Chemical free energy density

The chemical free energy density of a homogeneous system consisting of solid and liquid phases is decomposed into the chemical energy density associated with material composition and double-well potential energy

$$f^{chem}(\bar{c}_{Mg}, \phi) = (1 - h(\phi))f_l^{chem}(\bar{c}_{Mg}^l) + h(\phi)f_s^{chem}(\bar{c}_{Mg}^s) + \omega g(\phi), \qquad (2)$$

where $f_l^{chem}(\bar{c}_{Mg}^l)$ and $f_s^{chem}(\bar{c}_{Mg}^s)$ are the chemical free energy densities within the liquid and solid phases as a function of normalized phase-concentrations $\bar{c}_{Mg}^l$ and $\bar{c}_{Mg}^s$. In the above equation, $g(\phi)$ and $h(\phi)$ are the double-well potential energy and interpolation functions commonly expressed as

$$g(\phi) = 16\phi^2(1 - \phi)^2 \qquad h(\phi) = \phi^3(6\phi^2 - 15\phi + 10). \qquad (3)$$

ω in Eq. (2) is a constant that determines the energy barrier height at $\phi = 1/2$ between the two minima at $\phi = 0$ and $\phi = 1$. The chemical free energy densities within each phase in Eq. (2) are approximated by simple parabolic functions with the same curvature parameter A as

$$f_l^{chem}(\bar{c}_{Mg}^l) = \frac{1}{2}A(\bar{c}_{Mg}^l - \bar{c}_{Mg}^{l,eq})^2 \qquad f_s^{chem}(\bar{c}_{Mg}^s) = \frac{1}{2}A(\bar{c}_{Mg}^s - \bar{c}_{Mg}^{s,eq})^2, \qquad (4)$$

where $\bar{c}_{Mg}^{l,eq} = c_{Mg}^{l,eq}/c_{Mg}^s$ and $\bar{c}_{Mg}^{s,eq} = c_{Mg}^{s,eq}/c_{Mg}^s$ are the normalized equilibrium Mg concentrations in the liquid and solid phases. The interfacial region is defined as a mixture of both phases with different concentrations but with the same diffusion chemical potential

$$\bar{c}_{Mg} = (1 - h(\phi))\bar{c}_{Mg}^l + h(\phi)\bar{c}_{Mg}^s \qquad \frac{\partial f_l^{chem}(\bar{c}_{Mg}^l)}{\partial \bar{c}_{Mg}^l} = \frac{\partial f_s^{chem}(\bar{c}_{Mg}^s)}{\partial \bar{c}_{Mg}^s}. \qquad (5)$$

Using Eqs. (4) and (5) renders the following definition for the chemical free energy density of the system

$$f^{chem}(\bar{c}_{Mg}, \phi) = \frac{1}{2}A\left[\bar{c}_{Mg} - h(\phi)(\bar{c}_{Mg}^{s,eq} - \bar{c}_{Mg}^{l,eq}) - \bar{c}_{Mg}^{l,eq}\right]^2 + \omega g(\phi). \qquad (6)$$

Gradient energy density

The interfacial energy density is defined as

$$f^{grad}(\nabla\phi) = \frac{1}{2}\kappa|\nabla\phi|^2, \qquad (7)$$

where κ is the isotropic gradient energy coefficient. The phase-field parameters ω and κ are

connected to the interfacial energy Γ and interface thickness ℓ

$$\omega = \frac{3\Gamma}{4\ell} \qquad \kappa = \frac{3}{2}\Gamma\ell. \tag{8}$$

Strain energy density

Considering deformable elasto-plastic solids, the mechanical free energy density f^{mech} in Eq. (1) is additively decomposed into elastic f_e^{mech} and plastic components f_p^{mech}

$$f^{mech}(\nabla\mathbf{u}, \phi) = h(\phi)(f_e^{mech} + f_p^{mech}), \tag{9}$$

where $h(\phi)$ ensures the transition from the intact solid (uncorroded Mg alloy) to the completely corroded (liquid) phase. The elastic strain energy density f_e^{mech} is a quadratic form of the elastic strain

$$f_e^{mech}(\nabla\mathbf{u}) = \frac{1}{2}\boldsymbol{\varepsilon}^e : \mathbf{C} : \boldsymbol{\varepsilon}^e \qquad \boldsymbol{\varepsilon}^e = \boldsymbol{\varepsilon} - \boldsymbol{\varepsilon}^p, \tag{10}$$

where $\mathbf{C}$ is the rank-four elastic stiffness tensor and $\boldsymbol{\varepsilon}^e$ is the elastic strain tensor obtained by subtracting the plastic strain tensor $\boldsymbol{\varepsilon}^p$ from the total strain $\boldsymbol{\varepsilon}$. For linearized kinematics, the total strain tensor is the symmetric part of the displacement gradient

$$\boldsymbol{\varepsilon} = \frac{1}{2}(\nabla\mathbf{u} + (\nabla\mathbf{u})^T). \tag{11}$$

The elastic deformation of the solid is described by the isotropic linear elasticity theory so that the rank-four elastic stiffness tensor reads

$$C_{ijkl} = \lambda\delta_{ij}\delta_{kl} + \mu(\delta_{ik}\delta_{jl} + \delta_{il}\delta_{jk}), \tag{12}$$

where λ and μ are the Lamé elastic constants. The plastic strain energy density f_p^{mech} is incrementally computed from the plastic strain tensor $\boldsymbol{\varepsilon}^p$ and the Cauchy stress tensor $\boldsymbol{\sigma_0}$ for the intact configuration as

$$f_p^{mech} = \int_0^t \boldsymbol{\sigma_0} : \dot{\boldsymbol{\varepsilon}}^p \, dt. \tag{13}$$

Governing equations

The following time-dependent governing equations for the independent kinematic fields $\phi(\mathbf{x}, t)$, $\bar{c}_{Mg}(\mathbf{x}, t)$, and $\mathbf{u}(\mathbf{x}, t)$ are derived

$$\begin{cases} \dfrac{\partial \phi}{\partial t} = -L\Big(\dfrac{\partial f^{chem}}{\partial \phi} - \kappa \nabla^2 \phi\Big) \\[2mm] \dfrac{\partial \bar{c}_{Mg}}{\partial t} = -\nabla \cdot \mathbf{J}; \qquad \mathbf{J} = -D_{c_{Mg}}\nabla \bar{c}_{Mg} - D_{c_{Mg}} h'(\phi)(\bar{c}_{Mg}^{l,eq} - \bar{c}_{Mg}^{s,eq})\nabla \phi \\[2mm] \nabla \cdot \boldsymbol{\sigma} = \mathbf{0} \end{cases} \quad \text{in } \Omega, \qquad (14)$$

complemented with boundary conditions

$$\begin{cases} \kappa \mathbf{n} \cdot \nabla \phi = 0 \quad\text{and}\quad \mathbf{n} \cdot \mathbf{J} = 0 \quad \text{on } \partial\Omega \\[2mm] \mathbf{t} = \mathbf{n} \cdot \boldsymbol{\sigma} = \mathbf{t}^0 \quad \text{on } \partial\Omega_{\mathbf{t}} \quad\text{and}\quad \mathbf{u} = \mathbf{u}^0 \quad \text{on } \partial\Omega_{\mathbf{u}} \end{cases}. \qquad (15)$$

In the above equation, L is the kinetic coefficient that characterizes the interfacial mobility and $D_{c_{Mg}}$ the effective diffusion coefficient interpolated with the phase-field parameter between the phases

$$D_{c_{Mg}} = D_{c_{Mg}}^s h(\phi) + (1 - h(\phi))D_{c_{Mg}}^l, \qquad (16)$$

where $D_{c_{Mg}}^l$ and $D_{c_{Mg}}^s$ stand for the diffusion coefficients of Mg ions in the liquid (corrosive environment) and solid phases. $D_{c_{Mg}}^s \ll D_{c_{Mg}}^l$ is enforced to retard diffusion of Mg ions inside the solid phase. The role of mechanical fields on the interface kinetics is incorporated by modifying the interface mobility parameter L, which includes a mechano-electrochemical contribution that amplifies the dissolution process. Thus, the mechanical term $\partial f^{mech}/\partial \phi = h'(\phi)f^{mech}$ is neglected in the phase-field equation (Eq. (14)).

The role of mechanical fields in enhancing corrosion kinetics is incorporated by following Gutman's theory. The anodic dissolution can be amplified by an amplification factor that depends on local stress and strain distributions. As the anodic dissolution kinetics dictates interface motion, the interfacial mobility coefficient L is analogously connected to mechanical fields

$$\frac{L}{L_0} = \Big(\frac{\varepsilon^p}{\varepsilon_y} + 1\Big) \exp\Big(\frac{\sigma_h V_m}{RT}\Big), \qquad (17)$$

where L_0 is the interfacial mobility that physically corresponds to the anodic dissolution current i_0 in the absence of mechanical stresses and plastic strains.

Dimensional analysis

The governing equations Eq. (14) are normalized using the interface thickness ℓ as the characteristic length, Mg concentration in the solid phase c_{Mg}^s, diffusion coefficients of Mg ions in the liquid phase $D_{c_{Mg}}^l$, and the energy barrier height ω as the energy normalization factor.

The nondimensional time $\bar{t}$, nondimensional space coordinates $\bar{\mathbf{x}}$, and nondimensional gradient $\bar{\nabla}$ are given as

$$\bar{t} = \frac{tD^l_{c_{Mg}}}{\ell^2} \qquad \bar{\mathbf{x}} = \frac{\mathbf{x}}{\ell} \qquad \bar{\nabla} = \ell\nabla. \tag{18}$$

Other dimensionless fields and parameters are

$$\bar{c}_{Mg} = c_{Mg}/c^s_{Mg} \qquad \bar{c}^{l,eq}_{Mg} = c^{l,eq}_{Mg}/c^s_{Mg} \qquad \bar{c}^{s,eq}_{Mg} = c^{s,eq}_{Mg}/c^s_{Mg} \qquad \bar{D}_{c_{Mg}} = D_{c_{Mg}}/D^l_{c_{Mg}}$$

$$\bar{f}^{chem} = f^{chem}/\omega \qquad \bar{\boldsymbol{\sigma}} = \boldsymbol{\sigma}/\omega \qquad \bar{\kappa} = \kappa/(\omega\ell^2). \tag{19}$$

The above nondimensional variables return the following governing equations

$$\begin{cases} \dfrac{\partial \phi}{\partial \bar{t}} = -\tau\Big(\dfrac{\partial \bar{f}^{chem}}{\partial \phi} - \bar{\kappa}\bar{\nabla}^2\phi\Big) \\ \dfrac{\partial \bar{c}_{Mg}}{\partial \bar{t}} = \bar{\nabla} \cdot \Big[\bar{D}_{c_{Mg}}\bar{\nabla}\bar{c}_{Mg} + \bar{D}_{c_{Mg}}h'(\phi)(\bar{c}^{l,eq}_{Mg} - \bar{c}^{s,eq}_{Mg})\bar{\nabla}\phi\Big] \\ \bar{\nabla} \cdot \bar{\boldsymbol{\sigma}} = \mathbf{0}. \end{cases} \quad \text{in } \Omega, \tag{20}$$

along with the corresponding nondimensional boundary conditions.

2. COMSOL implementation

The resulting governing equations and accompanying boundary conditions are solved using the finite element software COMSOL Multiphysics [2]. To demonstrate the model implementation in COMSOL Multiphysics two different case studies are considered: Mg wires immersed in SBF in the absence of mechanical loading and Mg wires simultaneously immersed in SBF and subjected to tensile deformation along the wire axis. It is further assumed that the wire surface is protected against corrosion by a thin surface layer locally damaged in a small area. The initial breakdown of the protective layer enables the ingress of aggressive Cl^- ions leading to the nucleation of a pit that acts as a stress concentrator. The initial pit has a semi-circular shape with a radius of 10 μm around the whole diameter of the wire to maintain axisymmetric boundary conditions, Fig. 2.

The phase-field simulations are performed using an axisymmetric domain as illustrated in Fig. 2. The nondimensional form of governing equations (20) is solved with accompanying initial and boundary conditions. Due to symmetry, only half of the axisymmetric domain is considered in the simulation, as depicted in Fig. 2. To represent an unbounded domain, no flux (Neumann) boundary conditions are enforced at all the outer boundaries of the computational domain for both the phase-field and the Mg concentration. The protective film is modeled as an impermeable layer with a thickness of 0.5 μm around the wire surface with the corresponding

no flux boundary condition for both Mg concentration and phase-field.

The properties of the Mg alloy and parameters common to all phase-field simulations are listed in Table 1.
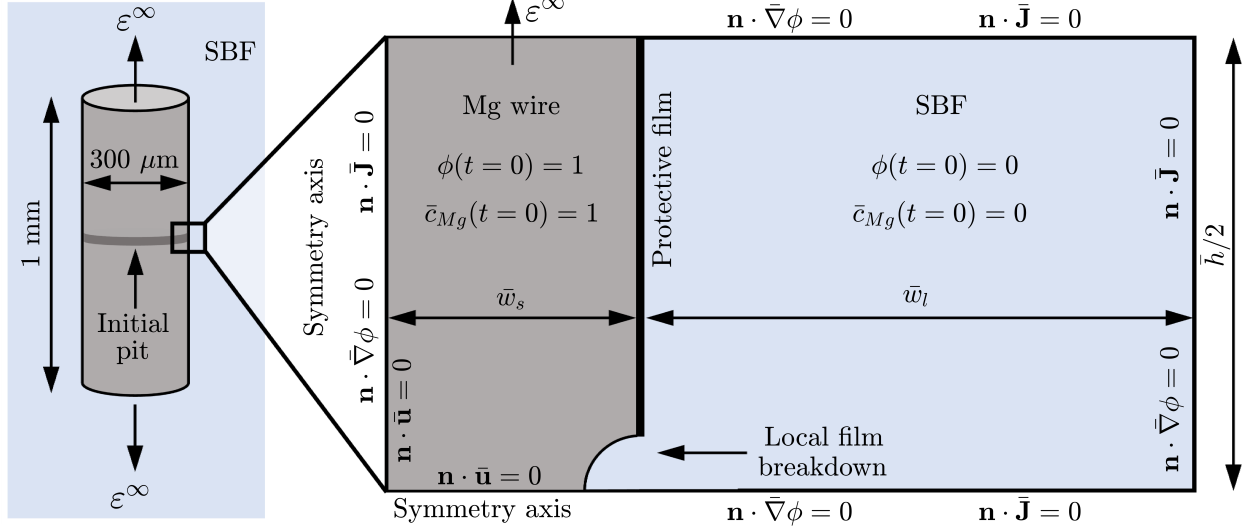

Figure 2: Simulation domain for the Mg alloy wire of 1 mm in length and 300 μm in diameter immersed in SBF and subjected to tensile deformation along the wire axis. The semi-circular pit created by the rupture of the protective layer has a radius of 10 μm. The size of the nondimensional computational domain ($\bar{w}_s = 37.5$, $\bar{w}_l = 362.50$, and $\bar{h} = 250$) is normalized using the interface thickness $\ell = 4$ μm as the characteristic length.

Quantity	Value	Unit
Diffusion coefficient of Mg ions in the liquid phase $D^l_{c_{Mg}}$	10^{-10}	m^2/s
Diffusion coefficient of Mg ions in the solid phase $D^s_{c_{Mg}}$	10^{-13}	m^2/s
Equilibrium concentration in the liquid phase $c^{l,eq}_{Mg}$	0.57	mol/L
Equilibrium concentration in the solid phase $c^{s,eq}_{Mg}$	71.44	mol/L
Molar volume of Mg V_m	13.998	cm^3/mol
Interfacial energy Γ	0.5	J/m^2
Interface thickness ℓ	4	μm
Chemical free energy density curvature parameter A	$6 \cdot 10^7$	J/m^3
Absolute temperature T	310.15	K

Table 1: Parameters common to all phase-field simulations.

2.1. Pitting corrosion

The governing equations for pitting corrosion (in the absence of mechanical loading) are

$$
\left.
\begin{cases}
\dfrac{\partial \phi}{\partial \bar{t}} = -\tau \Big(\dfrac{\partial \bar{f}^{chem}}{\partial \phi} - \bar{\kappa} \bar{\nabla}^2 \phi \Big) \\[3mm]
\dfrac{\partial \bar{c}_{Mg}}{\partial \bar{t}} = \bar{\nabla} \cdot \Big[\bar{D}_{c_{Mg}} \bar{\nabla} \bar{c}_{Mg} + \bar{D}_{c_{Mg}} h'(\phi)(\bar{c}^{l,eq}_{Mg} - \bar{c}^{s,eq}_{Mg}) \bar{\nabla} \phi \Big] \\[3mm]
\kappa \mathbf{n} \cdot \bar{\nabla} \phi = 0 \qquad \text{and} \qquad \mathbf{n} \cdot \bar{\mathbf{J}} = 0 \qquad \text{on } \partial \Omega
\end{cases}
\right\}
\tag{21}
$$

The primal kinematic variables are the phase field order parameter ϕ and the concentration of Mg $\bar{c}_{Mg}$. The `Mathematics` module with the `Coefficient Form PDE` and `General Form PDE`

interfaces is used to describe both equations [3]. The `Coefficient Form PDE` interface in the following form is used for the phase-field equation

$$e_a \frac{\partial^2 \phi}{\partial t^2} + d_a \frac{\partial \phi}{\partial t} + \nabla \cdot (-c\nabla\phi - \boldsymbol{\alpha}\phi + \boldsymbol{\gamma}) + \boldsymbol{\beta} \cdot \nabla\phi + a\phi = f \tag{22}$$

where the coefficients are chosen as $d_a = 1/\tau$, $c = \bar{\kappa}$, $e_a = a = 0$, and $\boldsymbol{\alpha} = \boldsymbol{\beta} = \boldsymbol{\gamma} = \mathbf{0}$ to represent the phase-field equation. The source term f is given as

$$f = \bar{A}\Big(\bar{c}_{Mg} - h(\phi)(\bar{c}_{Mg}^{s,eq} - \bar{c}_{Mg}^{l,eq}) - \bar{c}_{Mg}^{l,eq}\Big)(\bar{c}_{Mg}^{s,eq} - \bar{c}_{Mg}^{l,eq})h'(\phi) - \omega g'(\phi) + \bar{\kappa}\frac{\partial \phi}{\partial r}\frac{1}{r} \tag{23}$$

where the last term $\bar{\kappa}\frac{\partial \phi}{\partial r}\frac{1}{r}$ is added to take into account for the divergence operator in axisymmetric coordinates as this operation is not automatically included in `PDE Interfaces`.

The `General Form PDE` interface in the following form is used for the diffusion equation

$$e_a \frac{\partial^2 \bar{c}_{Mg}}{\partial t^2} + d_a \frac{\partial \bar{c}_{Mg}}{\partial t} + \nabla \cdot \Gamma = f \tag{24}$$

where the coefficients are chosen as $d_a = 1$ and $e_a = 0$ to represent the diffusion equation. The r and z components of the Γ vector are given as

$$\begin{aligned}
\Gamma_r &= -\bar{D}_{c_{Mg}}\frac{\bar{c}_{Mg}}{\partial r} - \bar{D}_{c_{Mg}}h'(\phi)(\bar{c}_{Mg}^{l,eq} - \bar{c}_{Mg}^{s,eq})\frac{\partial \phi}{\partial r} \\
\Gamma_z &= -\bar{D}_{c_{Mg}}\frac{\bar{c}_{Mg}}{\partial z} - \bar{D}_{c_{Mg}}h'(\phi)(\bar{c}_{Mg}^{l,eq} - \bar{c}_{Mg}^{s,eq})\frac{\partial \phi}{\partial z}
\end{aligned} \tag{25}$$

while the source term f includes the following term to account for the divergence operator in axisymmetric coordinates.

$$f = -\frac{\Gamma_r}{r}. \tag{26}$$

2.2. Mechanically-assisted corrosion

In addition to the above two equations for the phase-field parameter and the concentration of Mg, the `Solid Mechanics` interface is used to implement the governing equation for mechanical equilibrium

$$\left\{
\begin{aligned}
&\bar{\nabla} \cdot \bar{\boldsymbol{\sigma}} = \mathbf{0} \\
&\bar{\mathbf{t}} = \mathbf{n} \cdot \bar{\boldsymbol{\sigma}} = \bar{\mathbf{t}}^0 \qquad \text{on } \partial\Omega_{\mathbf{t}} \qquad \text{and} \qquad \bar{\mathbf{u}} = \bar{\mathbf{u}}^0 \qquad \text{on } \partial\Omega_{\mathbf{u}}
\end{aligned}
\right\}. \tag{27}$$

To investigate the influence of the mechanical fields on corrosion kinetics, additional constraints are enforced for the mechanical equilibrium equation. The normal component of the displacement

vector along the vertical and horizontal symmetry axes is constrained ($\mathbf{n} \cdot \bar{\mathbf{u}} = 0$) while a non-zero remote tensile deformation ε^∞ is prescribed on the top surface, Fig. 2. The remote deformation is prescribed at the beginning of the simulation and held fixed over a total simulation time.

The Mg alloy is assumed to behave as an isotropic, elasto-plastic solid. The Lamé elastic constants are $\lambda = 38$ GPa and $\mu = 16.3$ GPa. Plastic deformation is described using the J_2 flow theory with non-linear isotropic hardening, with a yield stress of 138 MPa and an ultimate tensile strength of 245 MPa at an engineering strain of 17%. The `Weak expression` of the governing equation (under the `Equation View` interface) is modified to account for the degradation of the material stiffness associated with the evolution of the corrosion front ϕ.

The `Solid Mechanics` interface computes and gives access to the effective plastic strain ε^p and the hydrostatic stress σ_h, which are required to enhance the phase-field mobility parameter in Eq. (17).

3. Numerical implementation

The computational domain of the Mg alloy and the surrounding physiological environment are discretized using triangular and quadrilateral finite elements (depending on the geometry considered) with second-order Lagrangian interpolation functions. To capture a smooth transition between the phase, we ensure that the interface thickness ℓ is at least five times smaller than the characteristic element size. This condition is fulfilled in all the simulations. To achieve that and to reduce computational costs, the mesh is only refined in the vicinity of the interface and the expected area of interface propagation; coarse mesh is kept far away from the interface. In addition, to execute simulations efficiently, an implicit time-stepping method is used for temporal discretization. The solver accuracy in each time step is controlled by a relative tolerance of 10^{-5}. The maximum time increment is constrained to $\Delta t = 50$ s in all the simulations (nondimensional time increment $\Delta \bar{t} = \Delta t D^l_{c_{Mg}}/\ell^2$). Further decreases in the time-step and mesh size in a convergence analysis show no impact on the outcome of the simulations.

4. Results

The results related to the above two case studies considered are given in this section for demonstration purposes. The interested reader is referred to the original paper [1] for more details and other case studies.

The obtained results in terms of phase-field contours, Mg concentration distribution, and mechanical fields for various remote deformations ε^∞ after 24 hours of immersion in SBF are

presented in Fig. 3. In the absence of mechanical loading ($\varepsilon^\infty = 0$), the pit grows uniformly, keeping the initial circular shape with a low and uniform concentration of Mg ions within the pit. The application of a relatively small axial deformation (e.g., $\varepsilon^\infty = 0.096\%$) increases the magnitude of σ_h in a small localized area and produces negligible plastic deformation. The hydrostatic stress distribution changes the pit morphology initiating a pit-to-crack transition. The Mg concentration increases near the tip of the pit, indicating that corrosion of Mg is localized in this region because of the stress concentration associated with the sharp tip. Further increase in the applied strain ($\varepsilon^\infty = 0.1\%$) raises the stresses high enough to trigger noticeable plastic deformations. The shape of the evolving defect is governed by both the hydrostatic stress and the plastic strain distribution. Longer and smoother cracks are observed compared to the previous case ($\varepsilon^\infty = 0.096\%$), as the hydrostatic stress and plastic strain distributions engage a more extensive area.
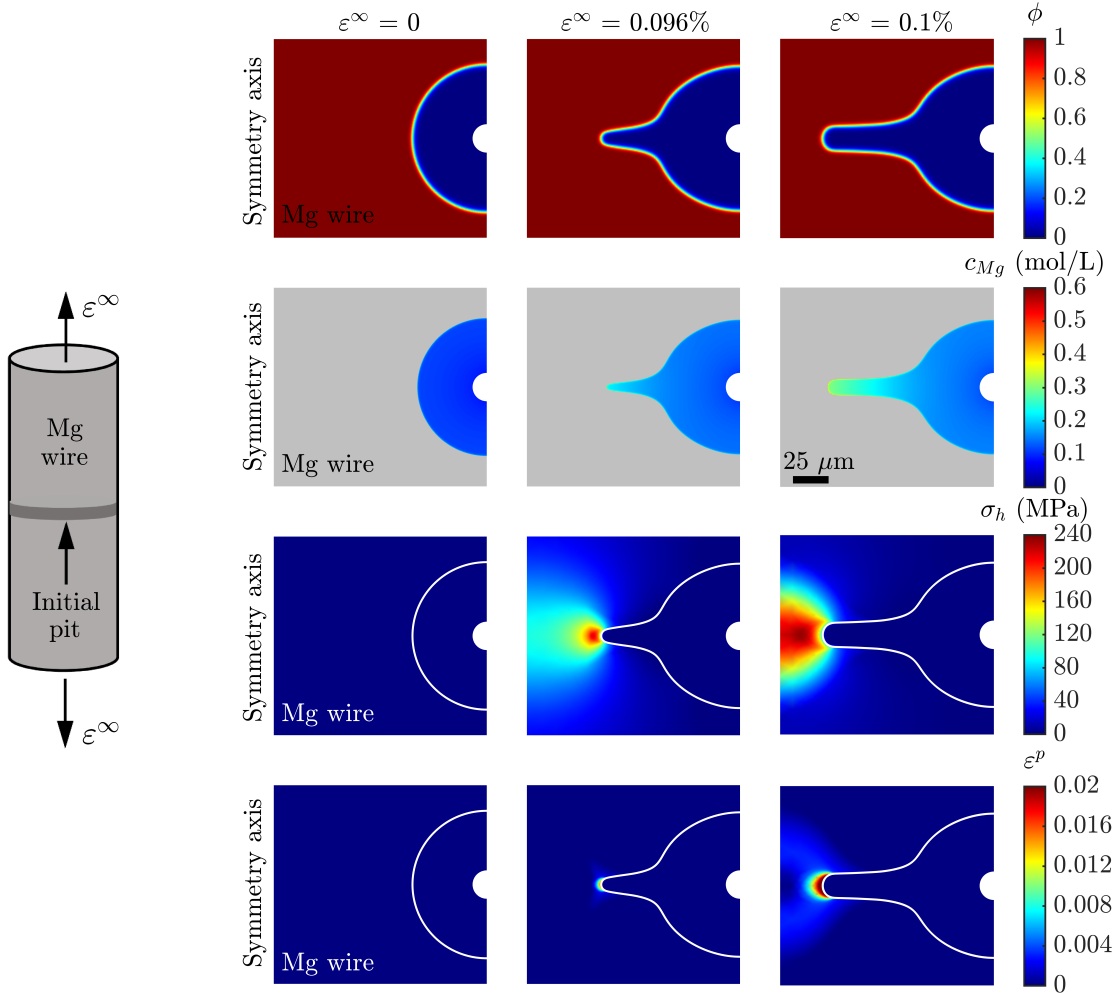

Figure 3: Contour plots of the phase-field variable, Mg concentration distribution in SBF, hydrostatic stress σ_h, and effective plastic strain ε^p for various prescribed remote deformations ε^∞ after 24 hours of immersion in SBF. The initial surrounding corrosive environment is not shown in the plots.

5. Concluding remarks

A finite element implementation of the phase-field model for simulating the corrosion of Mg alloys in body fluids developed by Kovacevic et al. (2023) is presented. The present document provides details of the model implementation in the software package COMSOL Multiphysics. Two case studies, namely pitting and mechanically-assisted corrosion, are explained in this document. The code developed is freely available at `www.imperial.ac.uk/mechanics-materials/codes`.

6. Acknowledgments

References

[1] S. Kovacevic, W. Ali, E. Martínez-Pañeda, J. LLorca, Phase-field modeling of pitting and mechanically-assisted corrosion of mg alloys for biomedical applications, Acta Biomater. 164 (2023) 641–658. `doi:https://doi.org/10.1016/j.actbio.2023.04.011`.

[2] COMSOL Multiphysics v. 5.6. www.comsol.com. COMSOL AB, Stockholm, Sweden.

[3] COMSOL Multiphysics v. 5.6. Reference Manual.